Vibrations of Euler's disk

Roberto Villanueva*
Department of Mechanical and Manufacturing Engineering, The University of Calgary, Calgary, Alberta T2N 1N4, Canada

Marcelo Epstein†
Department of Mechanical and Manufacturing Engineering, The University of Calgary, Calgary, Alberta T2N 1N4, Canada
(Received 8 February 2005; published 21 June 2005)

A model of a partially deformable Euler disk is presented that allows transverse vibrations to be treated with the techniques of classical analytical mechanics. The model clearly shows that the increasing audible frequency produced during motion can be directly related to the forcing effect of the reaction and the angular velocity of the contact point. The material of the disk seems to play a role in affecting the intensity and quality of the sound, but not its pitch. Moreover, the friction force grows rapidly with the decline of the disk, thus causing the slipping that is partially responsible for the abrupt end of the motion. The model also supports the conjecture [P. Kessler and O. M. O'Reilly, Regul. Chaotic Dyn. **7**, 49 (2002)] that the vibrations themselves contribute to this phenomenon by causing a loss of contact with the surface at small angles of inclination.

DOI: 10.1103/PhysRevE.71.066609 PACS number(s): 46.40.−f, 05.45.−a

I. INTRODUCTION

The familiar phenomenon of a coin rolling on a table gives rise to one of the classical problems of analytical mechanics with nonholonomic constraints (see, e.g., [1]). A toy of recent invention, known as Euler's disk [2], exhibits all the interesting features of this phenomenon. In particular, after a prolonged spinning motion, emitting a whirring sound of increasing frequency in the process, the disk comes to an abrupt stop. An article by Moffatt [3] proposing air viscosity as a mechanism for energy dissipation in Euler's disk generated numerous responses investigating aspects of his conjecture. Papers have been published supporting that solid friction, rather than viscosity in the air between the disk and surface, is the major source of energy dissipation (see Refs. [4–8]). Various articles also exist on the dynamics of the disk motion itself (see Refs. [9–13]). For the sake of brevity, the term "Euler's disk" is used in this paper to describe the general problem of rolling of a thin disk on a horizontal plane and does not refer to the specific geometry of the commercialized Euler's disk toy [2].

Kessler and O'Reilly [12] have presented a model of Euler's disk with an energy dissipation mechanism that considers both sliding and rolling friction. In the concluding comments, their article addresses two features of Euler's disk that merit attention. The first feature is the continuously increasing audible frequency that the disk produces as the angle of inclination declines. The model considered in [12], however, cannot capture the sound produced by the vibrations of the disk since it is based on rigid-body modeling. Nevertheless, the reaction force reported in the paper (cyclical and continuously increasing in frequency) is postulated as a measure of the forcing experienced by the disk (and surface) that can subsequently excite vibration and produce sound. The second feature is the abrupt stop of the motion of the disk. Kessler and O'Reilly [12] conjecture that, as the disk declines, the vibrations of the disk and surface eventually cause the disk to lose contact with the surface, thus abruptly ending the motion of the disk. They suggest that a deformable model for both the disk and surface is required to prove their conjecture.

Although experiments have been conducted to record the noise emitted from Euler's disk [11], to the best of our knowledge an analytical model that incorporates mechanical vibrations has not been proposed. In this paper, therefore, we attempt to address analytically the two features of Euler's disk underlined by Kessler and O'Reilly [12]. We suggest that in order to achieve a qualitatively correct description it is enough to use a single additional degree of freedom to represent the bending deformation of the disk. This approach is similar to that used in the theory of the so-called pseudorigid bodies [14,15]. When applied to a rolling disk, however, the pseudorigid-body formulation allows for in-plane vibrations of the disk (as shown in previous work by Cohen and Sun [16] and Epstein and Defaz [17]), but rules out the description of transverse bending vibrations. Our generalization, on the other hand, allows for transverse bending while preserving the main advantage of the pseudorigid approach: namely, a treatment within the realm of classical analytical mechanics rather than continuum mechanics. In other words, the model leads to a system of ordinary, instead of partial, differential equations. We hope that our model, albeit of partial deformability, will shed new light on some important aspects of the deformable Euler disk that have not been considered to date in the literature.

In Sec. II we derive the equations of motion and the constraints of the system, including the influence of rolling friction. In Sec. III we report and discuss the results of numerical simulations for our model under different types of rolling motion and their relation to the two points raised by Kessler and O'Reilly [12]. In Sec. IV we summarize the conclusions of our investigation.

*Electronic address: roberto_villanueva@yahoo.com
†Electronic address: mepstein@ucalgary.ca

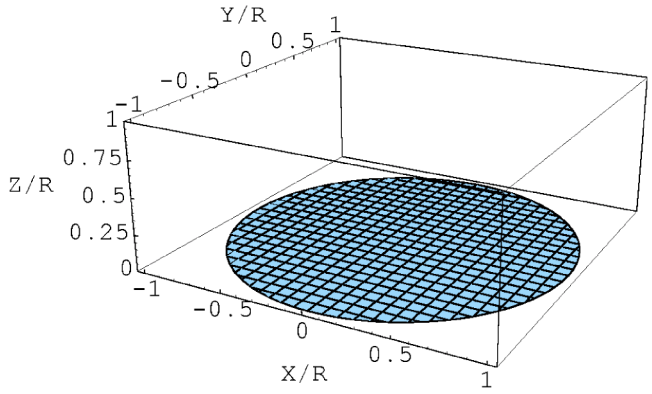

FIG. 1. Reference space: disk configuration in the "neutral" position.

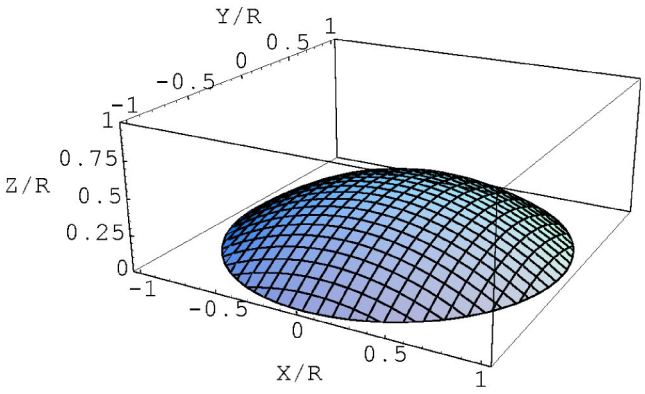

FIG. 2. Bending deformation of the disk.

II. DEFORMABLE DISK MODEL

A disk of constant thickness c and radius R (with $c/R \ll 1$) is assumed to lie in a reference space with Cartesian coordinates (X,Y,Z). The geometric center of the disk is at the origin and its middle surface lies in the plane $Z=0$ (Fig. 1). A deformation consists of a smooth placement of this disk in physical space, with coordinates (x,y,z). Assuming that the in-plane stiffness of the disk is much greater than its bending stiffness and recognizing that the bending deformations are likely to be small in comparison with the radius of the disk, we conclude that the most general deformation of interest consists of a field of small displacements normal to the disk superimposed on a general rigid-body motion of the latter. The generalized notion of pseudorigidity consists in further limiting the normal displacement field by prescribing that it must belong to a finite-parameter family of functions ("shape functions"). While this idea goes back to Rayleigh [18], it can also be considered as an example of a generalized constrained Cosserat point [19].

In the simplest possible version, the normal displacement field is controlled by a single shape function, which we will assume to be the following paraboloid:

$$f(X,Y) = 1 - \frac{1}{R^2}(X^2 + Y^2). \tag{1}$$

Accordingly, the actual normal displacement w (Fig. 2) is determined by a (small) time-dependent parameter $w_1(t)$, as follows:

$$w = w_1(t) f(X,Y). \tag{2}$$

Denoting by (x_1,y_1,z_1) the spatial location of the center of the disk and adopting a 3-1-3 set of Euler angles (ϕ,θ,ψ), also referred to as "type-II" Euler angles [20], the point (X,Y,Z) of the reference disk is mapped to the point in the deformed disk with spatial coordinates (x,y,z) given by

$$\begin{bmatrix} x \\ y \\ z \end{bmatrix} = \begin{bmatrix} x_1 \\ y_1 \\ z_1 \end{bmatrix} + \begin{bmatrix} a_{11} & a_{12} & a_{13} \\ a_{21} & a_{22} & a_{23} \\ a_{31} & a_{32} & a_{33} \end{bmatrix} \begin{bmatrix} X \\ Y \\ Z + w_1(t) f(X,Y) \end{bmatrix}, \tag{3}$$

where the rotation matrix is defined as

$$\begin{bmatrix} a_{11} & a_{12} & a_{13} \\ a_{21} & a_{22} & a_{23} \\ a_{31} & a_{32} & a_{33} \end{bmatrix} = \begin{bmatrix} \cos\phi & -\sin\phi & 0 \\ \sin\phi & \cos\phi & 0 \\ 0 & 0 & 1 \end{bmatrix} \begin{bmatrix} 1 & 0 & 0 \\ 0 & \cos\theta & -\sin\theta \\ 0 & \sin\theta & \cos\theta \end{bmatrix} \times \begin{bmatrix} \cos\psi & -\sin\psi & 0 \\ \sin\psi & \cos\psi & 0 \\ 0 & 0 & 1 \end{bmatrix}. \tag{4}$$

We are left with seven independent generalized coordinates as functions of time to fully describe the motion of the deformed disk: namely, x_1, y_1, z_1, ϕ, θ, ψ, and w_1.

To complete our model, we assume linear isotropic elasticity and constant density throughout the disk. The total kinetic energy of the disk is then given by

$$T = \int\int\int \frac{1}{2}\rho(\dot{x}^2 + \dot{y}^2 + \dot{z}^2) dX dY dZ,$$

where ρ is the density and where overdots indicate derivatives with respect to time t. Making the required substitutions, exploiting the thin-disk assumption, and carrying out the integration yields

$$\begin{aligned} T = \frac{\rho c \pi R^2}{24}\{&3R^2[\dot{a}_{11}^2 + \dot{a}_{12}^2 + \dot{a}_{21}^2 + \dot{a}_{22}^2 + \dot{a}_{31}^2 + \dot{a}_{32}^2] + 12[\dot{x}_1^2 + \dot{y}_1^2 \\ &+ \dot{z}_1^2] + 4[(w_1\dot{a}_{13} + \dot{w}_1 a_{13})^2 + 3\dot{x}_1(w_1\dot{a}_{13} + \dot{w}_1 a_{13})] \\ &+ 4[(w_1\dot{a}_{23} + \dot{w}_1 a_{23})^2 + 3\dot{y}_1(w_1\dot{a}_{23} + \dot{w}_1 a_{23})] \\ &+ 4[(w_1\dot{a}_{33} + \dot{w}_1 a_{33})^2 + 3\dot{z}_1(w_1\dot{a}_{33} + \dot{w}_1 a_{33})]\}. \end{aligned} \tag{5}$$

The potential energy due to gravity is easily evaluated as

$$V_g = \int\int\int \rho g z dX dY dZ = \frac{\rho c \pi R^2}{2}[w_1 a_{33} + 2z_1], \tag{6}$$

where g denotes the acceleration of gravity. Using standard assumptions in thin-plate elastodynamics [21] and denoting by E and ν, respectively, Young's modulus and Poisson's ratio, the stored elastic energy associated with the bending of the disk is obtained as

$$V_e = \int\int \frac{Ec^3}{24(1-\nu^2)}\left\{\left(\frac{\partial^2 w}{\partial X^2}+\frac{\partial^2 w}{\partial Y^2}\right)^2 - 2(1-\nu)\left[\frac{\partial^2 w}{\partial X^2}\frac{\partial^2 w}{\partial Y^2}-\left(\frac{\partial^2 w}{\partial X\,\partial Y}\right)^2\right]\right\} dX dY = \frac{\pi E c^3 w_1^2}{3(1-\nu)R^2}. \tag{7}$$

To impose the rolling constraint, we start by locating the point P along the perimeter occupying the lowest spatial position. Writing the parametric equations of the disk perimeter as $X=R\sin\gamma$, $Y=-R\cos\gamma$, $Z=0$, where γ is an angular parameter, a straightforward application of Eq. (3) yields the following expression for the z coordinate of points along the circumference:

$$z = z_1 + a_{31}R\sin\gamma - a_{32}R\cos\gamma.$$

Setting $\partial z/\partial\gamma=0$ and reading off a_{31} and a_{32} from Eq. (4), it follows that $\gamma_P=-\psi$, as expected on intuitive grounds. Since the condition of contact stipulates the vanishing of the z coordinate of the lowest point, we obtain the following (holonomic) constraint:

$$z_1 = R\sin\theta, \quad z_1 > 0,$$

which can also be written as

$$z_1^2 = R^2(a_{31}^2 + a_{32}^2). \tag{8}$$

Note that, by virtue of the assumed thinness, we impose the constraint at the middle surface of the disk. To enforce the no-slip condition of rolling, we further prescribe $\partial x/\partial t=0$ and $\partial y/\partial t=0$ at $\gamma=\gamma_P$. Using these conditions together with the result of Eq. (8) yields the following non-holonomic constraints:

$$\dot{x}_1 z_1 = R^2(\dot{a}_{11}a_{31} + \dot{a}_{12}a_{32}), \tag{9}$$

$$\dot{y}_1 z_1 = R^2(\dot{a}_{21}a_{31} + \dot{a}_{22}a_{32}). \tag{10}$$

Dissipation due to friction is modeled after the concept of a dissipative moment presented by Kessler and O'Reilly [12]. The dissipative moment $\mathbf{M}_f$ is conveniently expressed as

$$\mathbf{M}_f = -\sum_{i=1}^{3} \hat{\mathbf{a}}_i d_i \mathrm{sgn}(\boldsymbol{\omega}\cdot\hat{\mathbf{a}}_i), \tag{11}$$

where $\boldsymbol{\omega}$ is the disk rotational velocity and the basis $\hat{\mathbf{a}}_1$, $\hat{\mathbf{a}}_2$, $\hat{\mathbf{a}}_3$ is defined in terms of the basis $\hat{\mathbf{i}}$, $\hat{\mathbf{j}}$, $\hat{\mathbf{k}}$ of the x-y-z coordinate system, obtained after the first Euler rotation ϕ, as

$$\begin{bmatrix}\hat{\mathbf{a}}_1\\ \hat{\mathbf{a}}_2\\ \hat{\mathbf{a}}_3\end{bmatrix} = \begin{bmatrix}\cos\phi & \sin\phi & 0\\ -\sin\phi & \cos\phi & 0\\ 0 & 0 & 1\end{bmatrix}\begin{bmatrix}\hat{\mathbf{i}}\\ \hat{\mathbf{j}}\\ \hat{\mathbf{k}}\end{bmatrix}. \tag{12}$$

The parameters d_i are determined by factors such as the friction coefficient, the normal surface reaction force, and the contact area between the disk and surface. However, as we are not investigating the mechanism of rolling friction and are imposing a dissipative moment only to capture the qualitative aspects of dissipation in our model, we make the simplification that each d_i is constant.

Since the dissipative frictional forces do not derive from a potential, they must be included in Lagrange's equations of motion as generalized forces whose expressions are derived by means of the principle of virtual work [20]:

$$\delta W = \mathbf{M}_f\cdot\hat{\mathbf{e}}_\phi\delta\phi + \mathbf{M}_f\cdot\hat{\mathbf{e}}_\theta\delta\theta + \mathbf{M}_f\cdot\hat{\mathbf{e}}_\psi\delta\psi,$$

where the unit vectors $\hat{\mathbf{e}}_\phi$, $\hat{\mathbf{e}}_\theta$, and $\hat{\mathbf{e}}_\psi$ are defined in the directions of their respective rotation axes [20]. The resulting generalized forces are

$$\mathbf{Q}_\phi = \mathbf{M}_f\cdot\hat{\mathbf{e}}_\phi, \quad \mathbf{Q}_\theta = \mathbf{M}_f\cdot\hat{\mathbf{e}}_\theta, \quad \mathbf{Q}_\psi = \mathbf{M}_f\cdot\hat{\mathbf{e}}_\psi.$$

Similarly, dissipation due to structural damping in the disk material is considered by including a nonconservative generalized force $-\beta\dot{w}_1$ in the equation of motion for w_1. Quantitative investigation of the value of β is outside the scope of this paper as we are only interested in capturing the qualitative features of structural damping.

We form the Lagrangian $L=T-(V_g+V_e)$ and develop the equations of motion from an analytical approach. Constraints are enforced as generalized forces through the use of Lagrange multipliers λ_1, λ_2, and λ_3, corresponding to Eqs. (8), (9), and (10), respectively. The quantities λ_1, λ_2, and λ_3 are functions of time and represent the x, y, and z components, respectively, of the reaction force in physical space coordinates. The equations of motion for the unknown functions x_1, y_1, z_1, ϕ, θ, ψ, w_1, λ_1, λ_2, and λ_3 are

$$\frac{d}{dt}\left(\frac{\partial L}{\partial\dot{x}_1}\right) - \frac{\partial L}{\partial x_1} = \lambda_1, \tag{13}$$

$$\frac{d}{dt}\left(\frac{\partial L}{\partial\dot{y}_1}\right) - \frac{\partial L}{\partial y_1} = \lambda_2, \tag{14}$$

$$\frac{d}{dt}\left(\frac{\partial L}{\partial\dot{z}_1}\right) - \frac{\partial L}{\partial z_1} = \lambda_3, \tag{15}$$

$$\frac{d}{dt}\left(\frac{\partial L}{\partial\dot{\phi}}\right) - \frac{\partial L}{\partial\phi} = R\cos\theta(\lambda_1\cos\phi + \lambda_2\sin\phi) + \mathbf{M}_f\cdot\hat{\mathbf{e}}_\phi, \tag{16}$$

$$\frac{d}{dt}\left(\frac{\partial L}{\partial\dot{\theta}}\right) - \frac{\partial L}{\partial\theta} = R(-\lambda_1\sin\phi\sin\theta + \lambda_2\cos\phi\sin\theta - \lambda_3\cos\theta) + \mathbf{M}_f\cdot\hat{\mathbf{e}}_\theta, \tag{17}$$

$$\frac{d}{dt}\left(\frac{\partial L}{\partial\dot{\psi}}\right) - \frac{\partial L}{\partial\psi} = R(\lambda_1\cos\phi + \lambda_2\sin\phi) + \mathbf{M}_f\cdot\hat{\mathbf{e}}_\psi, \tag{18}$$

$$\frac{d}{dt}\left(\frac{\partial L}{\partial \dot{w}_1}\right) - \frac{\partial L}{\partial w_1} = -\beta \dot{w}_1. \tag{19}$$

When supplemented with the time-differentiated forms of Eqs. (8), (9), and (10), these equations constitute an algebraic-differential system defining our model of the deformable rolling disk.

III. NUMERICAL STUDIES

To carry out numerical simulations efficiently, the equations are nondimensionalized using the following variables:

$$\tilde{x}_1 = x_1/R, \quad \tilde{y}_1 = y_1/R, \quad \tilde{z}_1 = z_1/R, \quad \tilde{\phi} = \phi; \ \tilde{\theta} = \theta,$$
$$\tilde{\psi} = \psi, \quad \tilde{w}_1 = w_1/R, \quad \tilde{t} = kt, \quad \tilde{\lambda}_i = \lambda_i/(ERc),$$
$$\tilde{g} = g/(k^2 R),$$

where the "stiffness" parameter k is defined as

$$k = \sqrt{\frac{E\nu}{\rho c R}}. \tag{20}$$

All simulations were carried out using MATHEMATICA.

A. "Pseudosteady" motion

The initial conditions for steady motion of a rigid rolling disk have been previously investigated [10]. To initiate a "pseudosteady" type of motion (i.e., motion that is otherwise steady if not for the energy dissipation due to friction and vibration due to w_1), the same initial conditions will be applied. The required initial conditions are

$$\dot{\phi}^2 = \frac{g \cot\theta}{\frac{1}{4}R\cos\theta + \frac{3}{2}b}, \quad \dot{\psi} = -\dot{\phi}\left(\frac{b}{R} + \cos\theta\right), \quad \dot{\theta} = 0;$$
$$b > -\frac{1}{6}R\cos\theta,$$

where b is the initial horizontal distance from (x_1, y_1, z_1) to the center of the circle traced out by P during the motion.

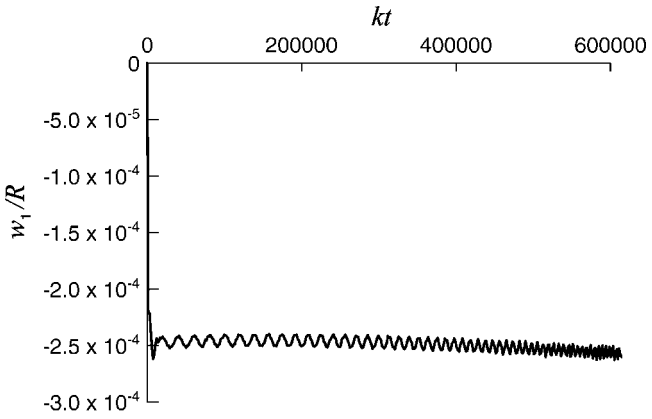

FIG. 3. Plot of w_1/R from $t=0$ to 16 s.

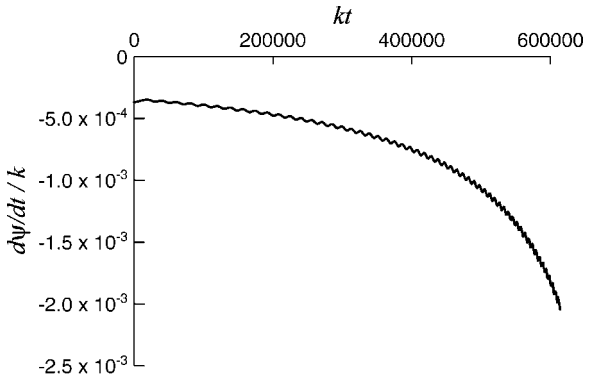

FIG. 4. Plot of $\dot{\psi}/k$ from $t=0$ to 16 s.

Example results are given for the following realistic conditions: $k=38\,383\ \mathrm{s}^{-1}$, $E=193$ GPa, $\rho=7860\ \mathrm{kg/m}^3$, $\nu=0.30$, $R=0.5$ m, $c=0.01$ m, $g=9.81\ \mathrm{m/s}^2$, initial coordinates of $P=(1,1,0)$m, initial $b=0$ m, initial $\phi=0°$, initial $\theta=20°$, initial $\psi=0°$, initial $w_1=0$, $d_1=30$ N m, $d_2=3$ N m, $d_3=0$ N m, and $\beta=100$ kg/s. Initial angular velocities are determined from the "pseudosteady" conditions above.

Figure 3 shows that in our deformable model, vibrations of the disk are indeed initiated. A plot (not shown) of w_1/R over a short time period reveals two prevalent frequencies. The first is the "forced frequency" observable in Fig. 3. This forced frequency increases as the angle of inclination of the disk θ decreases (i.e., as t increases). Conjecturing that the forced frequency would naturally arise from the time rate of change in γ_P (measure of "material" position of the contact point P) and recalling that $\gamma_P = -\psi$, we indeed find that the value of $\dot{\psi}$ (Fig. 4) correlates very well with the instantaneous frequencies inferred from Fig. 3 throughout the time period analyzed. The second frequency observed is the natural frequency of the disk (not observable in Fig. 3, as it is much higher than the forced frequency). The strength of the natural frequency is much smaller than the strength of the forced frequency (and it is in practice further mitigated by the structural damping of the disk). Although it would be interesting to analyze and compare Fig. 4 with the exponential fitting proposed by Caps *et al.* [8], the fact that our dissipation model is so coarse (constant moments) and that we did not pursue the detailed motion up to the last stages of

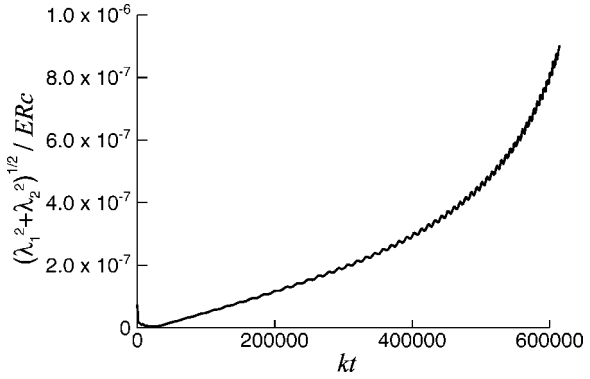

FIG. 5. Plot of the nondimensionalized magnitude of the friction force from $t=0$ to 16 s.

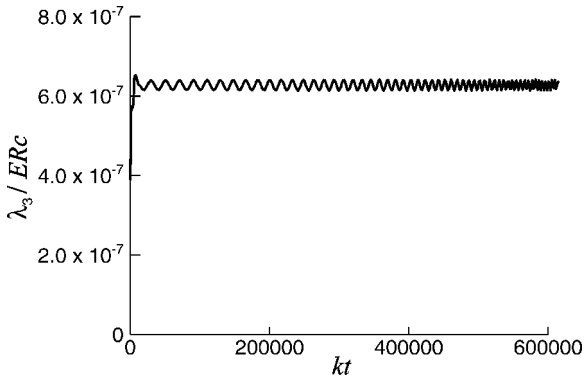

FIG. 6. Plot of nondimensionalized normal reaction force from $t=0$ to 16 s.

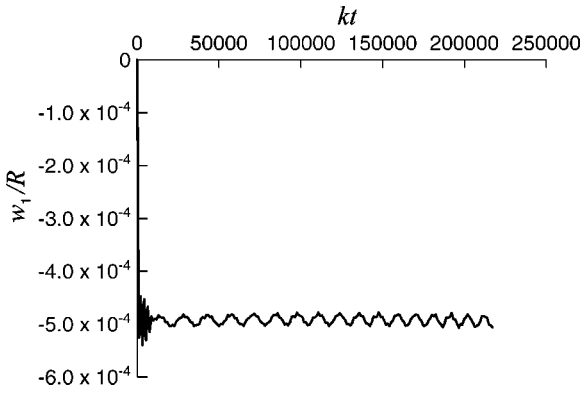

FIG. 8. Plot of w_1/R with $k=27141$ from $t=0$ to 8 s.

decline would make this exercise fruitless. Figures 5 and 6 show that both the friction and normal reaction forces on the disk increase in frequency as t increases. The frequency observed in these figures is, again, the forced frequency. We also note that Fig. 5 shows the magnitude of the friction force increasing with time. Figure 7 shows the movement of P over time is roughly circular, as expected with pseudosteady motion.

The first interesting feature of the Euler's disk problem raised by Kessler and O'Reilly [12] is the increasing audible frequency produced during the motion. With our deformable model for the disk, we can infer that the increasing forced frequency observed in the disk vibration and in the reaction force is a measure of the sound of increasing audible frequency produced during the motion. Although we assumed a rigid rolling surface, the forced frequency observed in the reaction force can be expected to play a similar role in inducing vibration in an actual deformable surface.

The second feature raised by Kessler and O'Reilly [12] is the abrupt end to the motion of the disk. While some authors [5,6] have reported experimental work showing rolling friction as the main factor of energy dissipation in the early stages of motion, experiments by Caps *et al.* [8] reveal that dissipation due to slipping is present in the latter stages of motion. The rapidly increasing magnitude of the friction force with time (Fig. 5) suggests that a threshold value for the friction force will be reached, beyond which the disk slips. Slipping might also be induced by the vibrations themselves through loss of contact with the surface, occurring more frequently and prominently at very small angles of inclination near the end of motion. The vibrations observed in our model appear to describe the vibrations conjectured by Kessler and O'Reilly [12] as causing the abrupt end to the motion.

Another interesting observation is the effect of stiffness on the vibration. For the same model parameters as used in Fig. 3, except that Young's modulus is reduced by one-half, Fig. 8 shows that the magnitude of the vibration increases. Nevertheless, the forced frequency observed in the vibration of the disk remains the same. This shows that the material seems to play a role in affecting the intensity and quality of the sound produced, but not its pitch.

B. Typical nonsteady motion

As pseudosteady initial conditions are not simple to implement in reality, we consider a typical nonsteady initial motion. This motion is based on imposing initial conditions of rotation about an axis running through P and (x_1,y_1,z_1) and has been previously considered by Kessler and O'Reilly [12]. A unit vector, $\hat{\mathbf{e}}_{P/1}$, is defined to describe this axis.

Example results are given for the following conditions: $k=38\,383\ \mathrm{s}^{-1}$, $E=193\ \mathrm{GPa}$, $\rho=7860\ \mathrm{kg/m}^3$, $\nu=0.30$, $R=0.5\ \mathrm{m}$, $c=0.01\ \mathrm{m}$, $g=9.81\ \mathrm{m/s}^2$, initial coordi-

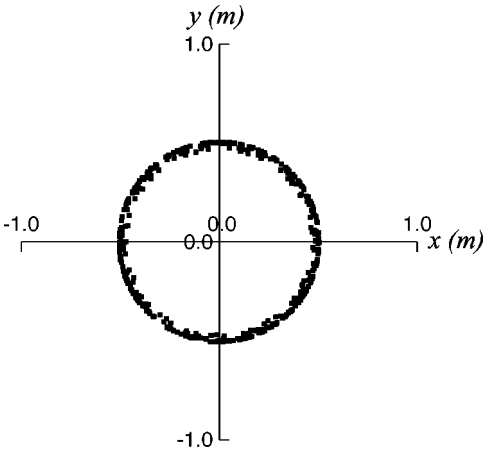

FIG. 7. x-y plot of P from $t=0$ to 16 s.

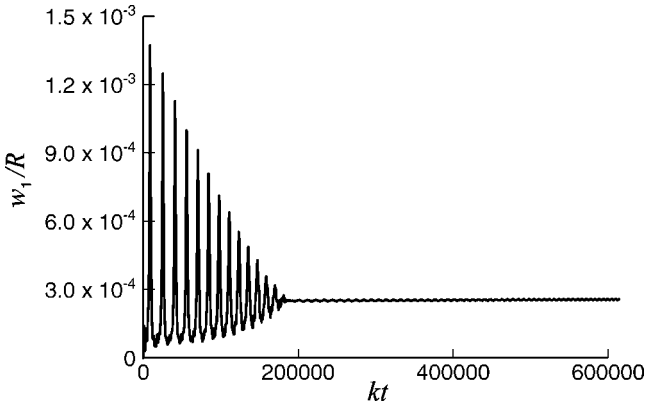

FIG. 9. $\boldsymbol{\omega}=-1.5\hat{\mathbf{e}}_{P/1}$; plot of w_1/R from $t=0$ to 16 s.

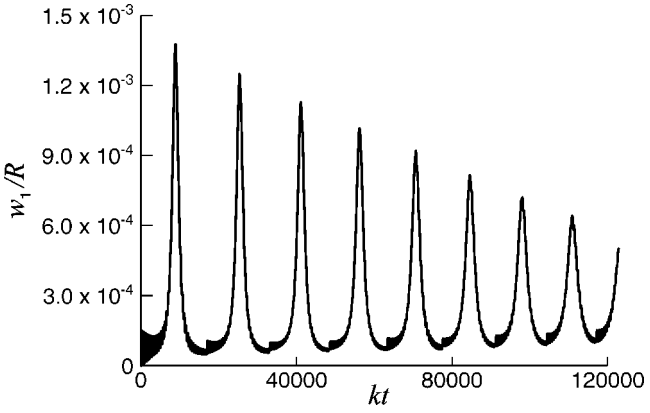

FIG. 10. $\boldsymbol{\omega}=-1.5\hat{\mathbf{e}}_{P/1}$; plot of w_1/R from $t=0$ to 4 s.

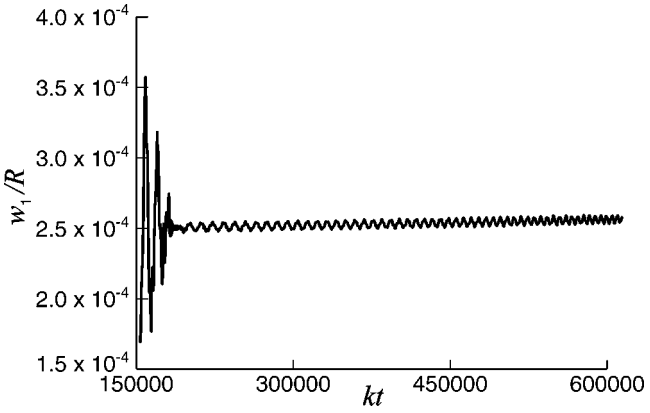

FIG. 11. $\boldsymbol{\omega}=-1.5\hat{\mathbf{e}}_{P/1}$; plot of w_1/R from $t=4$ to 16 s.

nates of $P=(1,1,0)$m, initial $\phi=0°$, initial $\theta=20°$, initial $\psi=0°$, initial $w_1=0$, $d_1=15$ N m, $d_2=1.5$ N m, $d_3=0$ N m, and $\beta=100$ kg/s. An initial angular velocity of $\boldsymbol{\omega}=-1.5\hat{\mathbf{e}}_{P/1}$ rad/s is studied.

A key observation from Figs. 9, 10, and 11 is that the typical nonsteady initial motion studied degenerates into pseudosteady motion as the angle of inclination of the disk θ decreases (i.e., as t increases). This corresponds well with the common observation of a coin or a dish eventually falling into a pseudosteady type of motion regardless of its initial conditions when first spun (reported experimentally by Easwar *et al.* [6]). At the start of the motion, the "forced frequency" observed is related to the nonsteady rising and falling of the disk. The magnitudes of the initial vibrations decrease as t increases. By the end of the motion, the "forced frequency" observed tracks well with $\dot{\psi}$ as already observed in the pseudosteady motion. In addition, as with the pseudosteady motion, the natural frequency of the disk is weakly present in the vibration. Thus, the comments made earlier on the interesting features of Euler's disk raised by Kessler and O'Reilly [12] also apply to the study of a typical nonsteady motion.

IV. CONCLUSION

A deformable model of the Euler's disk problem was developed by permitting the disk to deform in a prescribed shape. This approach allows the problem to be treated with the techniques of classical analytical mechanics. We attempted to address two interesting features of the Euler's disk problem raised by Kessler and O'Reilly [12]. Regarding the first feature—namely, the increasing audible frequency produced during motion—we observed that our deformable model captured a forced frequency in the disk vibration and in the reaction force that corresponds with the angular velocity of the contact point of the disk. This vibration and reaction force response can be interpreted as a measure of the sound produced during motion. The material seems to play a role in affecting the intensity and quality of the sound, but not its pitch. With respect to the second feature, the abrupt end to the motion of the disk, we observed friction force responses that support observations by others [8] of slipping occurring near the end of motion. The vibrations observed also support the conjecture by Kessler and O'Reilly [12] that vibrations could cause a loss of contact with the surface at small angles of inclination, contributing to an abrupt end of the motion. The concepts in this deformable model can be expanded upon to include flexibility in the rolling surface. Moreover, the methods introduced for prescribing a deformed shape for the disk can be used to explore higher modes of vibration excited in the disk. Carrying out these improvements may provide additional insight into the detailed mechanism and measure of sound produced during motion, but the general conclusions gathered from the present model are not likely to be affected.

ACKNOWLEDGMENTS

This work has been partially supported by the Natural Sciences and Engineering Research Council of Canada and the Alberta Heritage Scholarship Fund.

[1] Ju. I. Neimark and N. A. Fufaev, *Dynamics of Nonholonomic Systems* (American Mathematical Society, Providence, RI, 1972).
[2] J. Bendik *et al.*, US Patent No. 5,863,235, 1999.
[3] H. K. Moffatt, Nature (London) **404**, 833 (2000).
[4] G. van den Engh, P. Nelson, and J. Roach, Nature (London) **408**, 540 (2000).
[5] D. Petrie, J. L. Hunt, and C. G. Gray, Am. J. Phys. **70**, 1025 (2002).
[6] K. Easwar, F. Rouyer, and N. Menon, Phys. Rev. E **66**, 045102(R) (2002).
[7] L. Bildsten, Phys. Rev. E **66**, 056309 (2002).
[8] H. Caps, S. Dorbolo, S. Ponte, H. Croisier, and N. Vandewalle, Phys. Rev. E **69**, 056610 (2004).
[9] O. M. O'Reilly, Nonlinear Dyn. **10**, 287 (1996).
[10] A. J. McDonald and K. T. McDonald, e-print physics/0008227.

[11] A. A. Stanislavsky and K. Weron, Physica D **156**, 247 (2001).
[12] P. Kessler and O. M. O'Reilly, Regular Chaotic Dyn. **7**, 49 (2002).
[13] A. V. Borisov, I. S. Mamaev, and A. A. Kilin, Regular Chaotic Dyn. **8**, 201 (2003).
[14] J. J. Slawianowski, Arch. Mech. **26**, 569 (1974).
[15] H. Cohen and R. G. Muncaster, *The Theory of Pseudo-Rigid Bodies* (Springer-Verlag, Ann Arbor, MI, 1988).
[16] H. Cohen and Q. X. Sun, J. Sound Vib. **143**, 423 (1990).
[17] M. Epstein and I. Defaz, J. Appl. Mech. (to be published).
[18] J. W. S. Rayleigh, *Theory of Sound* (Dover, New York, 1976).
[19] O. M. O'Reilly, Int. J. Solids Struct. **35**, 1009 (1998).
[20] D. T. Greenwood, *Advanced Dynamics* (Cambridge University Press, Cambridge, England, 2003).
[21] L. D. Landau and E. M. Lifshitz, *Theory of Elasticity* (Pergamon Press, Bristol, 1975).